SEPARATION CONTROL BY SYNTHETIC JET ACTUATOR IN A STRAIGHT BLADE CASCADE

M. Matejka*, L. Popelka, P.Safarik*, J. Nozicka***
*** Department of Fluid Dynamics and Power Engineering, Faculty of Mechanical Engineering, Czech Technical University in Prague**
****Institute of Thermomechanics, Academy of science of the Czech Republic**

Keywords: *straight blade cascade, synthetic jet, flow visualization*

Abstract

The paper deals with an experimental research of active boundary layer control using periodic excitation by a synthetic jet on a straight compressor blade cascade flow. Synthetic jet was introduced on the side wall of the tunnel perpendicularly into the main flow just in position of leading edge of compressor blades. Visualizations of the flow field on the wall and total loss coefficient were obtained.

Nomenclature

F^+	[-]	nondimensional Frequency (Strouhal number)
Re	[-]	Reynolds number
St	[-]	Stokes number
P	[W]	input power
U_∞	[m s^{-1}]	main flow velocity
X_{te}	[m]	characteristic dimension
c	[m]	characteristic dimension, chord
$<c_{\mu}>$	[-]	unsteady component of momentum coefficient
d_h	[m]	hydraulic diameter
f	[Hz]	exciting frequency
h	[m]	width of slot of synthetic jet actuator
l	[m]	span of blade
$\dot{m}$	[kg s^{-1}]	mass flow rate
p_c	[kg m^{-1} s^{-2}]	total pressure
q	[kg m^{-1} s^{-2}]	dynamic pressure
s	[m]	spacing of blades
$\bar{u}_o$	[m s^{-1}]	mean velocity in the output orifice of the synthetic jet actuator
w	[J kg^{-1}]	specific work
α	[°]	reference incidence angle
α_2	[°]	output angle
δ	[°]	deviation
η_{sj}	[-]	efficiency of the synthetic jet
κ	[-]	error of measurement
ν	[m^2 s^{-1}]	kinematic viscosity
ζ	[-]	loss coefficient flow

1 Introduction

In the case of an off-design device operation, flow conditions are substantially changed. The flow separation considerably increases drag and reduces lift of the blades and consequently reduces the efficiency of turbomachines, Fig.1.

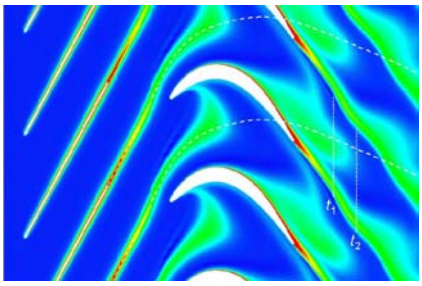

Fig. 1 Influence of wakes from the first to the second stage of turbomachines, numerical simulation, [1].

Similarly, the geometry of the area where the blade and the side wall of the channel are connected induces the creation of a secondary flow (vortices). Such structures usually have an unfavorable influence on the flow field of the channel and reduce the efficiency of the device, Fig. 2.

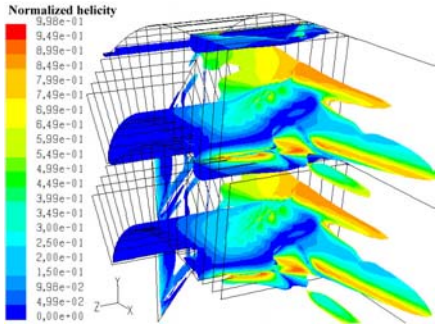

Fig. 2 Value of Normalized helicity inside a blade cascade, numerical simulation, [2].

The suppression of the flow separation can be carried out by using passive or active methods of the flow control. One of the most effective methods of an active flow control is the excitation by synthetic jet, applying zero mass-flux. The synthetic jet can affect the local and global structure of the flow field, namely acceleration of the transition from laminar to turbulent boundary layer, turbulent boundary layer separation, etc., [3] and [4]. The active flow control method is particularly effective in transport of mass and energy between the outer stream and the boundary layer.

1.1 Synthetic Jet

The synthetic jet can be produced by using an exciter (diaphragm) which is connected to a cavity which has an output orifice, see Fig. 3, [5].

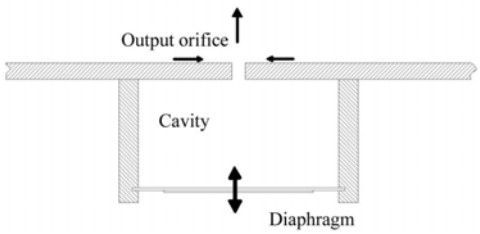

Fig. 3 Model of synthetic jet actuator.

The greatest effect is achieved when the output outlet is a rectangular slot. The principle of the synthetic jet is based on an alternate suction and blowing, which leads to the formation of vortices, [3], [4], [6]. In dependence mainly on the nondimensional frequency F^+ of synthetic jet, the vortices created by the synthetic jet cause either a gentle reduction or a growth of the shear layer (boundary layer). Using this principle, or an alternative such as an oscillating flap (surface), vortex structures are generated, which change the character of the shear layer.

Fundamental factors for the design of a synthetic jet actuator are nondimensional frequency F^+ (1), Stokes number of the output orifice St (2), Reynolds number of the output orifice Re_o (3), and $<c_\mu>$ unsteady component of momentum coefficient (4), [4], [5].

$$F^+ = \frac{f \cdot X_{te}}{U_\infty} \tag{1}$$

$$St = \frac{f \cdot h^2}{\nu} \tag{2}$$

$$\mathrm{Re}_o = \frac{\overline{u}_o \cdot d_h}{\nu} \tag{3}$$

$$c_\mu = \frac{\rho_o \cdot \int_0^h \overline{u}_o(y)^2 \, dy}{1/2 \rho_\infty U_\infty^2 c} \doteq \frac{\rho_o u_o'^2 h}{1/2 \rho_\infty U_\infty^2 c} \tag{4}$$

1.2 Loss coefficient

In order to obtain the influence of the synthetic jet to the flow field, loss coefficients must be defined, [7]. The local loss coefficient for the compressor blade cascade is defined by eq. (5):

$$\zeta(z) = \frac{p_{c1}(z) - p_{c2}(z)}{q_1(z = l/2)} \tag{5}$$

From the value of the local loss coefficient the values of the total loss coefficient, eq. (6), and the secondary loss coefficient, eq. (7) can be calculated.

$$\overline{\zeta}_T = \frac{2}{l} \int_0^{l/2} \zeta(z) dz \tag{6}$$

$$\overline{\zeta}_{3D} = \frac{2}{l} \int_0^{l/2} \left[\zeta(z) - \zeta_{l/2}(z) \right] dz \tag{7}$$

2 Influence of Synthetic Jet on the Flow Field

2.1 Model and Experimental Setup

Experiments were carried out on a straight compressor blade cascade consisting of 12

blades, Fig. 4, with following parameters: chord of blade $c = 72$ mm, span of blade $l = 160$ mm, angle of incidence of blade $\alpha = 5°$ and Reynolds number calculated from the chord of blade was set at $Re \cong 2 \cdot 10^5$. The outlet of the synthetic jet actuator was a slot with a variant width $h = 0.2$, 0.5 and 1 mm. Length of rectangular outlet (slot) corresponding with spacing of blades $s = 36$ mm. The synthetic jet actuator outlet was placed on the side wall at the level of leading edges of blades perpendicular to the main flow, Figs. 4 and 5. The compressor blade cascade and synthetic jet actuator were placed in a low speed Eiffel-type aerodynamic tunnel with a test section of 160 mm width and 300 mm height.

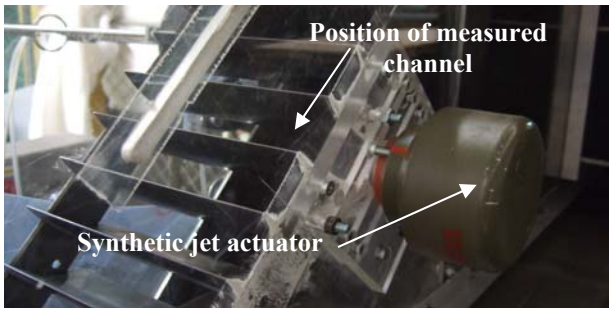

Fig. 4 Position of the synthetic jet actuator

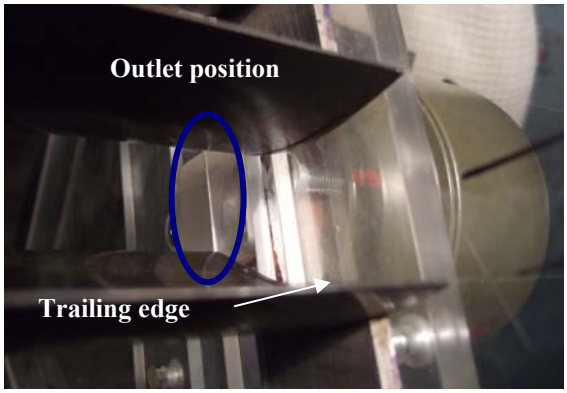

Fig. 5 Straight blade cascade and active actuator layout.

With respect to nondimenzional frequency F^+, Stokes number St and Reynolds number of output slot, the exciting frequency f of the synthetic jet Re_o was changed from $f = 600$ Hz to $f = 1000$ Hz by 200 Hz in sequence.

Tab. 1 shows values of the unsteady part of momentum coefficient $<c_\mu>$ calculated from the main flow velocity $U_\infty = 44$ m/s and chord of blade c. The value of momentum coefficient c_μ calculated at exciting frequency $f = 1200$ Hz and the width of slot $h = 0.2$ mm is too low to affect the flow field sufficiently. The value of nondimensional frequency F^+ for exciting frequency $f = 300$ Hz is outside of optimal interval $F^+ \approx 1$ to 2. Due to the mentioned reasons above, exciting frequency f of the synthetic jet was adjusted to $f = 0$, 600, 800 and 1000 Hz. For detailed information about characteristics of the synthetic jet actuator and its flow conditions please refer to the literature [8].

$<c_\mu>$ [1]	h [mm]		
f [Hz]	0.2	0.5	1
300	0.00087	0.00248	-
600	0.00094	0.00240	0.00091
800	0.00072	0.00199	0.00069
1000	0.00047	0.00169	0.00084
1200	0.00024	0.00119	0.00082

Tab. 1 Value of unsteady part of momentum coefficient $<c_\mu>$ for defined conditions.

2.2 Data Obtained from Pressure Measurement and Flow Visualization

The local loss coefficient $\zeta(z)$ for the compressor blade cascade was calculated from data obtained from the five-hole pneumatic probe under conditions mentioned above. For all exciting frequencies and slot widths values of the total loss coefficient, eq. (6), and the secondary loss coefficient, eq. (7) were determined. The local loss coefficient was measured in six sections, at a distance of $\Delta z = 20$, 30, 40, 50, 60 and 80 mm from the side wall of the tunnel (span-wise direction, Fig. 6).

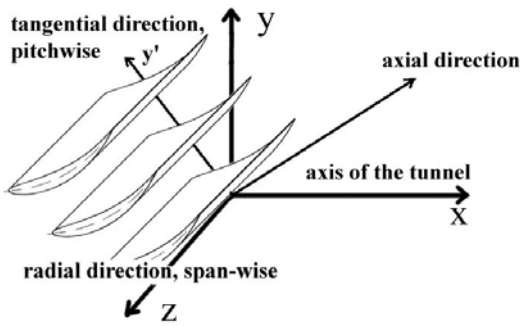

Fig. 6 Coordinate System

All obtained data were normalized by the value excluding the influence of the synthetic

jet. Tab. 2 and 4 show normalized values of total and secondary loss coefficient in dependency on the exciting frequency and the width of slot. Their proportional changes are shown in Tab. 3 and 5. Note that the outlet of the synthetic jet actuator is placed on the side wall of the tunnel. In spite of the big distance of the first measuring section from the side wall of the tunnel $z = 20$ mm there is a significant influence to the losses.

	f [Hz]			
h [mm]	0	600	800	1000
0.2	1	0.9933	0.9865	0.9825
0.5	1	1.0167	1.0049	0.9965
1	1	1.0132	0.9970	0.9962

Tab. 2 Normalized value of total loss coefficient

	f [Hz]			
h [mm]	0	600	800	1000
0.2	0	-0.67	-1.36	-1.75
0.5	0	1.67	0.48	-0.36
1	0	1.32	-0.28	-0.38

Tab. 3 Proportional change of total loss coefficient [%]

	f [Hz]			
h [mm]	0	600	800	1000
0.2	1	0.9634	0.9487	0.9407
0.5	1	1.0257	0.9938	0.9680
1	1	1.0154	0.9771	0.9727

Tab. 4 Normalized value of secondary loss coefficient

	f [Hz]			
h [mm]	0	600	800	1000
0.2	0	-3.66	-5.13	-5.93
0.5	0	2.57	-0.62	-3.20
1	0	1.54	-2.29	-2.73

Tab. 5 Proportional change of secondary loss coefficient [%]

The flow pattern was visualized by an oil film method under identical conditions as mentioned above for width of slot $h = 0.2$ mm. Changes in a deviation of the flow and the development of the wake on the side wall, highlighted in red, are shown in Fig. 7. The green color highlights the development of the secondary flow near the side wall. The positive influence of higher exciting frequency on an extent of the wake, change of deviation and secondary flow direction are clearly visible.

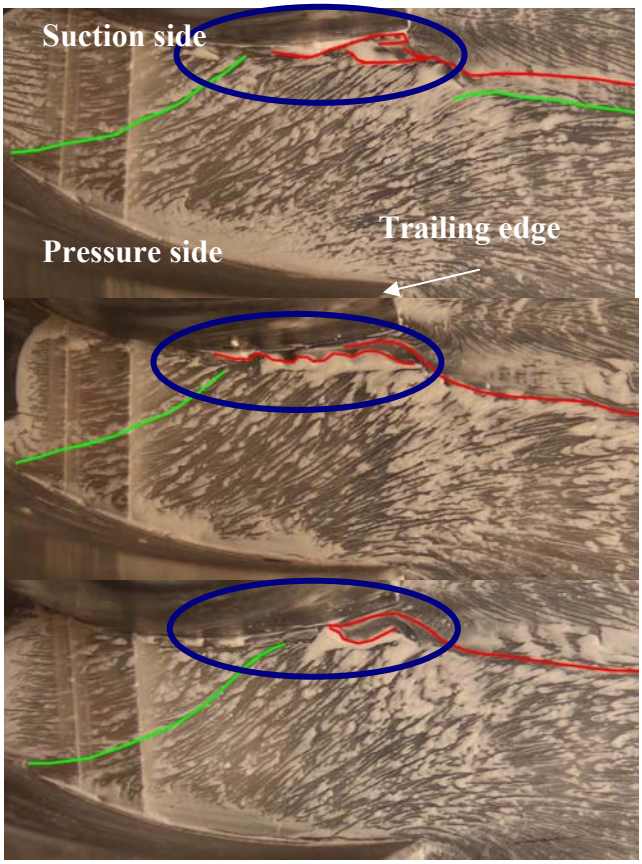

Fig. 7 Visualization of the side wall of the tunnel, excitation frequency $f = 0$, 600 and 1000 Hz (from the first to the last)

The red color, on the pressure side of the blade, indicates the position of the sudden boundary layer transition, see Fig. 8. The green color sets off the boundary layer transition on the pressure side of the blade under the effect of the vortex structures near the side wall of the tunnel. The effect of exciting frequency of the synthetic jet is identical to the one mentioned in the previous case. Due to a higher exciting frequency of the synthetic jet, the boundary layer transition near the side wall was delayed.

Figure 9 shows the influence of the synthetic jet on the suction side of the blade. Red line marks the line between the main flow and the separated flow. Green lines underline the flow inside the separated zone. The blue circle emphasizes a continuous area inside the separated zone. In this case, size of continuous area was reduced through the higher exciting frequency of the synthetic jet.

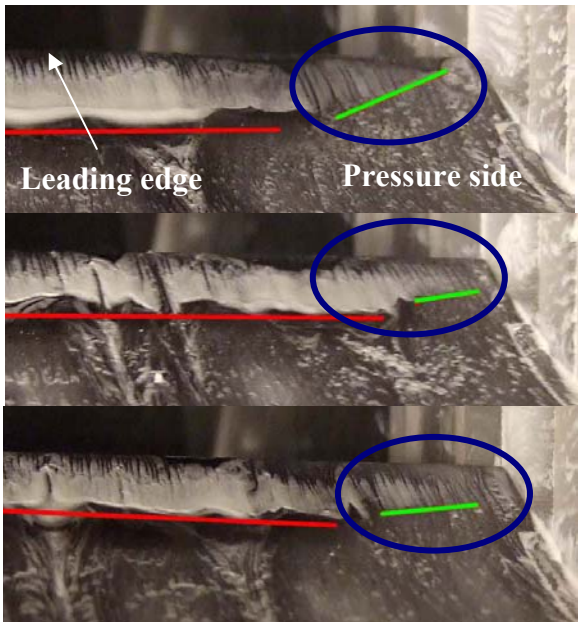

Fig. 8 Visualization of the pressure side of the blade, excitation frequency f =0, 600 and 1000 Hz, (from the first to the last)

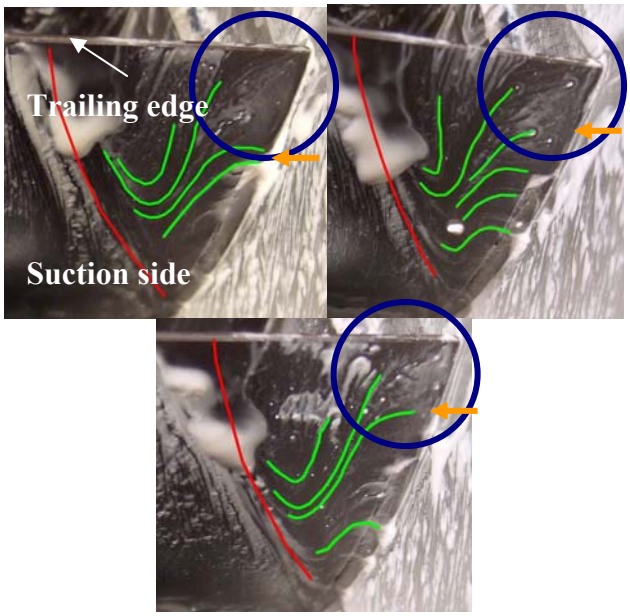

Fig. 9 Visualization of the suction side of the blade, excitation frequency f = 0, 600 and 1000 Hz, (from the first to the last)

3 Discussion

As a result, an appreciable influence of the synthetic jet on the flow field was proved, although the synthetic jet affected only a relatively small part of the flow field. Data obtained from measurements on the five tube cone pressure probe reveal that a decrease of the total loss coefficient by 1.8 % and of the secondary loss coefficient by 6 % were achieved, see Tables 3 and 5. The flow visualization proved noticeable positive effect of the synthetic jet to the flow field near the side wall. A change of the extent of the wake, the position of boundary layer transition and the flow structure in separated zone are evident. Positive influence of higher exciting frequency is obvious.

Further, based on the data obtained from the five tube cone pressure probe measurement, the deviation of main flow was calculated. Fig. 10 shows the difference between the values of deviation of the main flow calculated with and without considering the influence of the synthetic jet. However, due to the measured value and the measurement error $\kappa_\alpha = \pm 0.4°$ of the output angle $\alpha_2(z)$ (deviation δ), the discussion regarding this results can not be completed. Nevertheless, a considerable impact of the slot dimension and the excitation frequency of the synthetic jet on the flowfield formation is clearly visible. It results from the above, that a lower excitation frequency and a wider slot width caused a greater deviation.

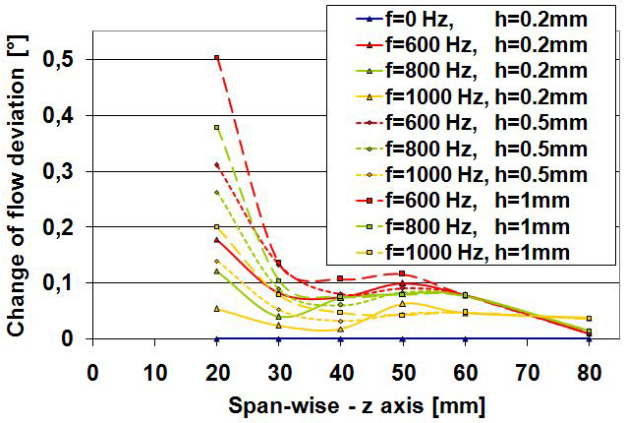

Fig. 10 Influence of slot dimension and excitation frequency of synthetic jet on the change in flow deviation.

The values of the excitation frequency and the Stokes number of the output orifice of the synthetic jet actuator have a significant effect on the value of the loss coefficients. Tables 2 and 4 show a positive influence of the rising excitation frequency of the synthetic jet on the total and secondary loss coefficient. The positive impact of a low value output slot Stokes number is also clearly apparent in Tables 2 and 4. It can be

observed that the loss coefficients are considerably influenced at the lower level of Stokes numbers.

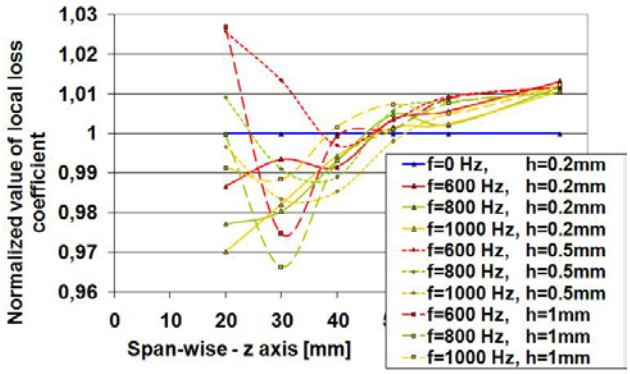

Fig. 11 Development of the normalized value of the local loss coefficient along the span of the blade with respect to the excitation frequency, width of slot $h = 0.2$, 0.5 and 1 mm.

In order to determine the magnitude of the loss coefficients the measurement error must be defined. The measurement error of the total and secondary loss coefficient is 0.8% of its absolute value. Fig. 11 shows the behavior of the local loss coefficients depending on the position of the section along the span of the blade at various exciting frequencies and widths of slot h. A considerable decrease can be observed in the local loss coefficient near the side wall. This decrease is caused by the influence of the synthetic jet. Despite detailed analyses of results of measurements, the cause of the growth of the local loss coefficient in the central position of the span blade was not determined. With respect to the measurements uncertainty (0.8 %), the growth of local loss coefficient is low.

Fig. 12 shows the normalized value of the total loss coefficient, including the measurement uncertainty in relation to the exciting frequency. As far as the measurement uncertainty is concerned, it can be noted that a reduction in the total loss coefficient was achieved.

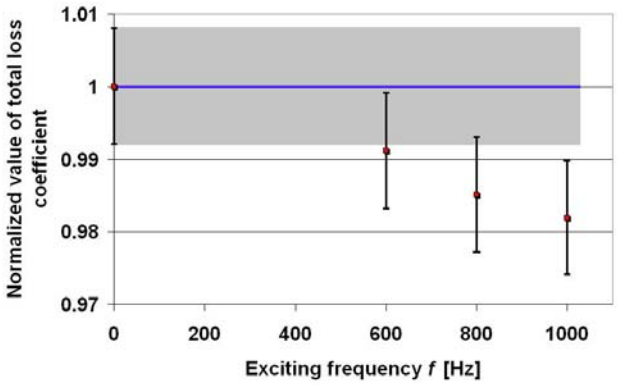

Fig. 12 Normalized value of the total loss coefficient with respect to the excitation frequency, width of slot $h = 0.2$.

Further, there is another very important aerodynamic parameter which is the ratio of axial velocity – AVR (flows with insignificant change of density), eq. 8, ref. [9]. Values of AVR for the width of slot $h = 0.2$ mm and all exciting frequencies are shown in Tab. 6.

$$AVR = \frac{v_{ax2}}{v_{ax1}} \tag{8}$$

	$h = 0.2$ mm			
f [Hz]	0	600	800	1000
AVR	1.2603	1.2608	1.2621	1.2627

Tab. 6 *AVR*

There are not substantial changes of AVR in relation to the exciting frequency. The changes of AVR are negligible compared to the value of the measurement error. The same data were obtained from flow visualization, see Fig. 10 above.

A comparison of the values of the theoretical secondary loss coefficient $\bar{\zeta}_{3D\,theor.}(f)$, eq. (9), and the real (measured) secondary loss coefficient $\bar{\zeta}_{3D\,real}(f)$ for width of slot $h = 0.2$ mm is presented in Tab. 7. It is visible that the maximum saving of the total loss coefficient $\bar{\zeta}_T$ (about 1.8 %) corresponds to the theoretical decrease of secondary loss coefficient $\bar{\zeta}_{3D\,theor.}(1000)$ at about 4,3 %. The maximal difference between real $\bar{\zeta}_{3D\,real}(f)$ (11) and theoretical secondary coefficient is about 1.5%. That is probably caused by the change of the flow structure

inside the separated zone (the suction side of the blade near the side wall).

$$\bar{\zeta}_{3D\,theor.}(f) = \bar{\zeta}_T(f) - \left[\bar{\zeta}_T(0) - \bar{\zeta}_{3D}(0)\right] \tag{9}$$

$$\bar{\zeta}_{3D\,theor.}(f)[\%] = \frac{\bar{\zeta}_{3D\,theor.}(f) - \bar{\zeta}_{3D}(0)}{\bar{\zeta}_{3D}(0)} \tag{10}$$

$$\bar{\zeta}_{3D\,real}(f)[\%] = \frac{\bar{\zeta}_{3D\,real.}(f) - \bar{\zeta}_{3D}(0)}{\bar{\zeta}_{3D}(0)} \tag{11}$$

	f [Hz]			
loss	0	600	800	1000
$\bar{\zeta}_T(0) - \bar{\zeta}_{3D}(0)$	0.069	0.069	0.069	0.069
$\bar{\zeta}_{3D\,theor.}(f)$	0.0457	0.0450	0.0441	0.0437
$\bar{\zeta}_{3D\,theor.}(f)$[%]	0	-1.68	-3.39	-4.33
$\bar{\zeta}_{3D\,real}(f)$	0.0457	0.0440	0.0434	0.0430
$\bar{\zeta}_{3D\,real.}(f)$[%]	0	-3.66	-5.14	-5.93

Tab. 7 Change of theoretical and real secondary loss coefficient. Width outlet of slot h = 0.2 mm.

3.1 Efficiency of the synthetic jet

A crucial role in flow control plays an evaluation of the influence of the synthetic jet on the flow field considered from the view of energy transformations. Therefore, an amount of input energy to the losses must be compared. The specific work loss w_{loss} can be calculated from the total loss coefficient and the input value of the main flow velocity, eq. (12). The specific saved up work w_s can be formulated from the difference of the total loss coefficients with and without the influence of the synthetic jet, eq. (13).

$$w_{loss} = \bar{\zeta}_T \cdot \frac{1}{2} \cdot U_\infty^2 \tag{12}$$

$$w_s = \left[\bar{\zeta}_T(0) - \bar{\zeta}_T(f)\right] \cdot \frac{1}{2} \cdot U_\infty^2 \tag{13}$$

$$w_{add} = \frac{P}{\dot{m}} \tag{14}$$

$$\eta_{sj} = \frac{w_{add} - w_s}{w_{add}} \tag{15}$$

From the relation of the input electric power P to the mass flow $\dot{m}$ in the controlled region (the blade channel) the specific added work, eq. (14) can be obtained. The efficiency of the synthetic jet η_{sj}, eq. (15) is defined by the ratio of difference between the added work and the specific saved up work to the specific added work. The efficiency of the synthetic jet expresses how much energy is saved in relation to the added energy. Tab. 8 shows the ranges of efficiency of the synthetic jet for all possible excitation frequencies and slot widths. The maximum efficiency of the synthetic jet η_{sj} = -0.84 is achieved at the excitation frequency f = 1000 Hz and Stokes number St = 2.7, width of slot h = 0.2 mm. In this case, almost 2 more times saved up energy was obtained in relation to the added energy.

η_{sj}	f [Hz]			
h [mm]	0	600	800	1000
0.2	1	0.28	-0.44	-0.84
0.5	1	2.74	1.51	0.63
1	1	2.48	0.66	0.57

Tab. 8 Efficiency of synthetic jet η_{sj} for all possible excitation frequencies and slot widths.

4 Conclusions

The experimental results show a significant effect of synthetic jet actuator on the loss coefficients value. For total and secondary loss coefficient, reductions of nearly 2% and 6% respectively, were achieved. The extent of the saving noticeably depends on the optimal value of nondimensional characteristics of the synthetic jet such as a nondimensional frequency F^+, Stokes number St and momentum coefficient c_μ.

The efficiency of a synthetic jet η_{sj} was defined, considering the effectiveness of the

flow control. In this case, the best value of synthetic jet efficiency η_{sj} = -0.84 was obtained. This means that there was nearly two more times saved up energy in relation to the added energy.

The position of the output slot of the synthetic jet also has an appreciable effect on the value of the loss coefficient. A decrease in the secondary loss coefficient was achieved because the output slot was situated on the side wall of the tunnel. A more considerable effect on the total loss coefficient would be achieved by positioning the output slot of the synthetic jet generator directly on the blade (along the span of the blade). However, there are technological problems with installing this equipment directly on a thin blade.

Acknowledgment

This work has been supported by the project of Progressive Technology System for Power Engineering 1M06059, by the Ministry of Education, Youth and Sports of the Czech Republic No. 1M06031. Grant support from GA AS of the Czech Republic No. A2076403, No. A200760614 is also gratefully acknowledged.

References

[1] Praisner T. J., Clark J. P., Nash T.C., Rice M. J., Grover E. A. (2006): Performance Impact due to Wake Mixing in Axial-Flow Turbumachinery, ASME Turbo Expo 2006, GT2006-90666

[2] Simurda (2005): Vortex structure into blade cascades. Czech Technical University in Prague, FME. Graduation theses, in Czech.

[3] Greenblatt D., Wygnanski I. J. (2000): The Control of Flow Separation by Periodic Excitation. Aerospace Science 36 (2000), pp. 487-545.

[4] Glezer, A., Amitay, M. (2002): Synthetic Jet. Annual Revision Fluid Mechanics 2002, 34.

[5] Uruba, V (2005): Flow control using synthetic jet actuators, Eng. Mech. 12 (1) (2005), pp. 41–62.

[6] Matejka, M., Souckova, N. Popelka, L., Nozicka, J. (2007): Active Flow Control on the Simplified Flapped Airfoil. 1st CEAS European Air and Space Conference, Berlin, p. 237–241.

[7] Cumpsty, N. A. (1989): Compressor Aerodynamics. Longman Group UK Limited 1989.

[8] Matejka, M., Popelka, L., Safarik, P., Nozicka, J. (2008): Influence of Active Methods of Flow Control on the Compressor Blade Cascade Flow, ASME Turbo Expo 2008, Berlin, GT2008-51109

[9] Gostelow, J., P.: Cascade Aerodynamics. Pergamon Press Ltd, Oxford, England, 1984.

Copyright statement